Real-space description of current-constrained molecular junctions

Anna Painelli*
Dipartimento Chimica GIAF, Parma University, 43100 Parma, Italy
and INSTM UdR Parma, 43100 Parma, Italy

(Received 7 April 2006; revised manuscript received 15 May 2006; published 5 October 2006)

A current constrained approach is proposed for the calculation of characteristic current/voltage curves for molecular junctions described in a real space representation. A steady-state current is imposed on the molecule prepared in a nonequilibrium state, and the voltage drop is obtained from the electrical power spent on the molecule to sustain the current. The molecular resistance is related to relaxation phenomena that drive the molecule towards the equilibrium state. A phenomenological model, borrowed from the field of molecular spectroscopy, is adopted to describe relaxation, accounting for both depopulation and dephasing (inelastic and elastic scattering). The current is related to coherences, and the coherence lifetimes, with contributions from both depopulation and dephasing, enter the definition of the molecular resistance. For the specific case of a single electron in a two-site junction the standard result of conductivity quantization is regained, a result that holds for dispersionless as well as dispersive junctions. The proper implementation of the continuity constraint for steady-state dc transport requires the introduction of multiple Lagrange multipliers and results in nonlinear potential profiles across the molecule leading to the intriguing concept of bond resistance.

DOI: 10.1103/PhysRevB.74.155305 PACS number(s): 73.63.−b, 85.65.+h, 71.10.Fd

I. INTRODUCTION

Molecular junctions are complex systems where a molecule, an intrinsically microscopic object, is contacted by macroscopic leads.[1–3] To sustain the current the junction must be prepared in a nonequilibrium state: work has to be spent on the system to sustain the current and, to guarantee for steady-state conditions, exactly the same amount of work must be dissipated to the environment.[4] The most popular approaches to describe molecular junctions are based on the Bütticker-Landauer picture:[5–7] the junction, i.e., the molecule possibly including atoms from the contact region, is embedded between two semi-infinite electrodes that act as the source and the sink for the electrons. The electrical flux is driven by imposing a finite potential drop between the two electrodes to enforce a net flux of charges from the high to the low potential region. This voltage constrained (VC) approach proved very successful in the description of mesoscopic and nanoscopic junctions and has been quite naturally combined with detailed first-principles models for the molecular structure and the contact region.[1] However, working with infinite reservoirs poses some fundamental physical problems,[8–12] among which the need to account, in the same quantum mechanical system, for two families of electrons with different chemical potential, and, henceforth, the need to rely on one-electron models for the electronic structure.

To overcome the problem of semi-infinite reservoirs, Di Ventra and Todorov[13] recently proposed an interesting picture where a quasistationary current flows between two large but finite electronic reservoirs. The approach relies on the definition of a finite system with open boundary conditions, but the price to be paid is that a genuine steady state cannot be attained. Any reference to reservoirs is avoided in current constrained (CC) approaches that have been developed to describe transport in both meso- and molecular junctions.[8,12,14–18] Closed boundary conditions are imposed to the system, and a current is forced through the circuit, via some physical or mathematical device. CC and VC approaches are therefore complementary and, in a sense, describe two different experiments, where either the current or the potential drop is fixed from the outset.[14]

On physical grounds a current can be forced in a circuit by driving a time-dependent magnetic flux through the circuit. The model, originally proposed by Kohn to describe optical conductivity in extended systems,[19] has been applied to describe electrical transport in mesoscopic systems,[8,15] and more recently in molecular junctions.[18] Alternatively, variational techniques can be adopted, and the system can be forced in a nonequilibrium steady state introducing properly defined Lagrange-multipliers in the Hamiltonian. Again this technique has a long history in the field of mesoscopic transport[14] and has been more recently adopted to describe molecular junctions.[12,16,17]

CC approaches overcome the problem of reservoirs and, not relying on single-electron pictures, quite naturally apply to correlated electrons.[12,14] Whereas CC strategies are promising, two main problems remain to be solved: (1) the calculation of the potential drop needed to sustain the current, and (2) the definition of the potential profile in the molecule. To solve the first problem I take advantage from energy conservation as described by the Joule law: in a system with fixed current, the potential drop can be obtained from the electrical work done on the junction to sustain the current. The calculation requires of course a model for the relaxation dynamics: this is an important observation since it points out the fundamental link between resistance and relaxation. Charge-conservation is the key to solve the second problem: enforcing the continuity constraint for DC transport leads to the definition of the potential profile along the junction. The approach is general: here I sketch its application to linear Hubbard chains. Fully exploiting the possibility to account for correlations, I describe transport adopting a real space representation for the molecule leading to a suggestive picture where the molecule is described as an electrical circuit with resistances associated with chemical bonds.

Section II introduces the method with reference to the simplest case of a two-site junction. Section III extends the

discussion to polyatomic junctions: the continuity constraint for DC transport is introduced, showing that it defines nonlinear potential profiles through the junction. In the last section main results are discussed and summarized.

II. THE TWO-SITE JUNCTION

To start with consider a diatomic Hubbard molecule, whose Hamiltonian is defined by U, t, and the difference of on-site energies, $2\Delta=\epsilon_2-\epsilon_1$, as follows:

$$H_0=\epsilon_1\hat{n}_1+\epsilon_2\hat{n}_2+t\sum_{\sigma}(c_{1\sigma}^{\dagger}c_{2\sigma}+\text{H.c.})+U(\hat{n}_{1,\alpha}\hat{n}_{1,\beta}+\hat{n}_{2,\alpha}\hat{n}_{2,\beta}), \quad (1)$$

where $c_{i,\sigma}^{\dagger}$ creates an electron with spin σ on the i-site and $\hat{n}_i=\Sigma_\sigma\hat{n}_{i,\sigma}=\Sigma_\sigma c_{i,\sigma}^{\dagger}c_{i,\sigma}$. The eigenstates of H_0 are stationary states and do not sustain any current. To impose a finite steady-state current the molecule must be prepared in a nonequilibrium state $|G(\lambda)\rangle$ that can be defined (in the low temperature limit) as the ground state of the auxiliary Hamiltonian:[14,17]

$$H(\lambda)=H_0-\lambda\hat{j}, \quad (2)$$

where $\hat{j}=-i\Sigma_\sigma(c_{1\sigma}^{\dagger}c_{2\sigma}-\text{H.c.})$ measures the current flowing through the bond. Here and in the following e, $\hbar$, and t are adopted as units for charge, momentum, and energy, respectively. The field λ coupled to the current enters the Hamiltonian as a Lagrange multiplier, whose value is fixed by the requirement that a finite current $J=\langle G(\lambda)|\hat{j}|G(\lambda)\rangle$ flows through the molecule. $H(\lambda)$ is defined for a fixed number of electrons: global charge conservation is an obvious constraint for steady-state DC current, and cyclic boundary conditions are implied in the Lagrange multiplier approach, so that any electron escaping the molecule from the right immediately enters the molecule from the left side.

The same cyclic boundary conditions are adopted in the description of molecular junctions recently proposed by Burke *et al.*[18] In that case the molecule is embedded into an ideal conducting ring and, following Kohn,[19] a magnetic flux oscillating at frequency ω is driven through the ring as to generate a spatially uniform oscillating electric field E along the molecule. As discussed by Maldague in a different context,[20] at the leading order in the vector potential, the molecular Hamiltonian reduces to Eq. (2), with λ proportional to the amplitude of the vector potential. At least for the two-site molecule the Lagrange multiplier approach represents the low-λ limit of the Kohn model.

Both the Hubbard Hamiltonian in Eq. (1) and its current-carrying version in Eq. (2) can be diagonalized using standard real space techniques. The real space basis is defined by the complete set of orthonormal functions that specify the occupation of local (site) spin-orbitals (in other words the basis functions correspond to the Slater determinants written on the basis of the site spin-orbitals).[21] The Hamiltonians conserve the spin, so that subspaces with different spin numbers are decoupled. Here I will always work in the subspace relevant to the ground state, i.e., that defined by the wave functions with S_z (the z-component of the total spin) fixed at the lowest value ($S_z=0$, corresponding to singlet states, for an even number of electrons, $S_z=1/2$, corresponding to doublet states, for an odd number of electrons).[21,22] Two electrons in the two-site junction can then be described by the four basis states, $|\uparrow\downarrow,00\rangle$, $|00,\uparrow\downarrow\rangle$, $|\uparrow 0,0\downarrow\rangle$, and $|0\downarrow,\uparrow 0\rangle$, where 0 represents an unoccupied spin orbital, and the arrows represent up and down spins. The dimensions of the problem increase fast with the number of sites,[21,22] but the relevant matrix can be written and diagonalized numerically for not too large systems.[21,22] The valence bond basis, the linear combination of the real-space functions that diagonalize both S_z and S^2, represents a more efficient choice,[22] but the calculations become more involved due to the loss of orthogonality.

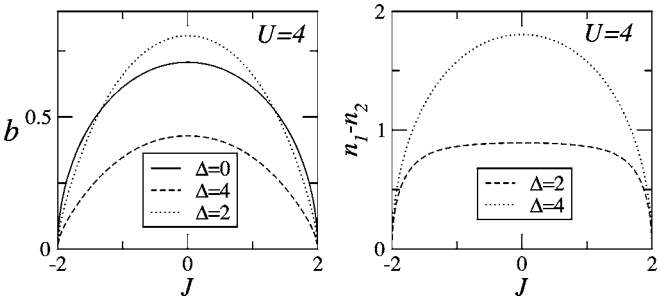

FIG. 1. The bond order and the difference of on-site electronic population as a function of the current flowing in a two-site two-electron Hubbard junction with $t=1$, $U=4$, and variable Δ.

The (numerically) exact diagonalization of the $H(\lambda)$ matrix, written on the real space basis, leads to the relevant ground state wave function $|G(\lambda)\rangle$, that, according to the previous discussion, describes a molecule carrying a finite current, $\langle G(\lambda)|\hat{j}|G(\lambda)\rangle$. Expectation values of other operators on the same state give important information on the effects of the current on molecular properties: the Lagrange multiplier approach offers an easy route to investigate the chemical effects of a DC current. Just as an example, for the two-site junction described by the Hamiltonians in Eqs. (1) and (2), I will shortly address the effects of the current on the charge distribution. On-site electron densities are the expectation values of the number operators, $\hat{n}_1$ and $\hat{n}_2$, and since the total number of electrons is fixed, the only relevant information is given in terms of $n_1-n_2=\langle G(\lambda)|\hat{n}_1-\hat{n}_2|G(\lambda)\rangle$, the unbalance in the electron number. Symmetry imposes $n_1-n_2=0$ for $\Delta=0$, irrespective of λ. The right panel of Fig. 1 shows the J dependence of n_1-n_2 for a two-site junction with two electrons, $t=1$, $U=4$ and two different Δ values. In both cases n_1-n_2 decreases with the (absolute value of) the current: when the current flows, electrons are more homogeneously distributed. This result can be easily understood since J increases with λ, and the effect of a finite Δ in $H(\lambda)$ becomes less and less important with increasing λ. The bond-order $\hat{b}=\Sigma_\sigma(c_{1\sigma}^{\dagger}c_{2\sigma}+\text{H.c.})/2$ measures the electron density between the two sites, and hence the strength of the chemical bond. Results in the left panel of Fig. 1 show that for all Δ, the expectation value $b=\langle G(\lambda)|\hat{b}|G(\lambda)\rangle$ decreases with increasing current: as electrons contribute to the current

their contribution to the chemical bond decreases. This is an interesting result since it suggests a lengthening of chemical bonds due to the current flow. This concept, however, is rooted in the adiabatic representation of the coupled electronic and vibrational motion and relies on the hypothesis of conservatives forces in current carrying nonequilibrium systems.[23] Both hypothesis deserve attention.

The definition of characteristic current-voltage curves requires the calculation of the potential drop needed to sustain the current. Of course λ is related to the field driving the current, and hence to the potential drop, but sorting out the relation is far from trivial. In the low-λ limit, where the Lagrange multiplier corresponds to the vector potential, the relevant electric field $E \propto \omega\lambda$ vanishes in the $\omega=0$ DC limit, leading to the unphysical result of a finite current driven through the system at zero bias. This zero-resistance picture emerges because scattering events or relaxation processes are totally disregarded. Indeed a finite potential drop is needed to sustain the current just because the current must overcome some friction in the junction. Any reliable calculation of characteristic curves must rely on the definition of a model for scattering or relaxation.

In single-electron pictures electrical resistance is naturally described in terms of scattering events: the electron traveling in the device undergoes elastic and/or inelastic scattering when impinging on scattering centers that may include phonons, electrodes, and possibly other electrons. In correlated pictures, the same phenomenon is described in terms of the relaxation of (multielectron) molecular eigenstates. To be specific, the current-carrying state $|G(\lambda)\rangle$ is a nonequilibrium state and the system relaxes back to the ground $|G(0)\rangle$ state. The amount of power spent to sustain the system in the nonequilibrium current-carrying state is set by the relaxation dynamics: the faster the relaxation the more power must be spent to sustain the current. The Joule law quantitatively defines the relation between the electrical power spent on the molecule, W, and the potential drop needed to sustain the current: $W=JV$. Since J is known, characteristic $J(V)$ curves can be obtained from W.

Following standard approaches in molecular spectroscopy, relaxation is conveniently described introducing the density matrix written on the basis of the eigenstates $|k\rangle$ of $H(0)$.[24,25] The equilibrium density matrix for the molecule in the absence of the driving field, σ_0, is a diagonal matrix whose elements are fixed by the Boltzmann distribution. In the low temperature limit only the lowest eigenstate, $|G(0)\rangle = |g\rangle$, is populated. In nondegenerate systems $\hat{j}$ is an off-diagonal operator, so that $\sigma(\lambda)$, the density matrix for the nonequilibrium system, is nondiagonal: finite *coherences*, i.e., nonvanishing off-diagonal elements of the density matrix, are needed to describe a current.

Our description of the molecular junction focuses on the electronic degrees of freedom of the molecule: σ represents a reduced density matrix, obtained from the complete density matrix by tracing out *bath* degrees of freedom, including those related to, e.g., vibrations and leads. The Liouville equation, the dynamical equation for the density matrix, must then be extended as follows: $\dot{\sigma}=-i[H,\sigma]+\dot{\sigma}_R$, where $\dot{\sigma}_R$ accounts for relaxation phenomena, as due to the coupling of the molecule to the bath.[24,25] Diagonal elements of $\dot{\sigma}_R$ describe variation of populations. A simple phenomenological model for population dynamics, borrowed from spectroscopy,[24,25] sets

$$(\dot{\sigma}_R)_{kk} = \sum_m \gamma_{km}\sigma_{mm} - \sum_m \gamma_{mk}\sigma_{kk}, \tag{3}$$

where γ_{km} measures the probability of the transition from m to k. Since k and m states are nondegenerate, the transition occurs only if the bath degrees of freedom can accept or provide the relevant energy: diagonal elements of $\dot{\sigma}_R$ correspond to processes where energy is exchanged between the system and the bath, i.e., they describe *inelastic* scattering processes. In the low-temperature limit, only downwards transitions occur: $\gamma_{km}=0$ for $k>m$, the bath can only accept energy from the system.

As for coherences, i.e., off-diagonal elements of σ, the standard expression for relaxation dynamics is given in terms of an inverse lifetime for each coherence, Γ_{km}, as follows:[24,25]

$$(\dot{\sigma}_R)_{km} = -\Gamma_{km}\sigma_{km}. \tag{4}$$

Two contributions enter Γ_{km}:

$$\Gamma_{km} = (\gamma_{kk} + \gamma_{mm})/2 + \gamma'_{km}, \tag{5}$$

where $\gamma_{kk}=\Sigma'_m\gamma_{mk}$ measures the inverse lifetime of state k as due to inelastic scattering (depopulation). So the first term in Γ_{km} comes from inelastic scattering: since the population of states k and m changes with time the relevant coherence is damped. The second contribution, γ'_{km}, is not related to the relaxation of populations but just describes the loss of coherence due to *dephasing*. Dephasing accounts for relaxation phenomena that do not require any exchange of energy with the bath, i.e., it accounts for *elastic* scattering processes.[24,25] I underline that, whereas this model for relaxation dynamics is purely phenomenological, it obeys basic physical requirements (including detailed balance), it is general and properly underlines the different roles of depopulation and dephasing or elastic and inelastic scattering.[24,25]

We are now in the position to evaluate the electrical power spent on the molecule to sustain the current:

$$W = -\lambda\,\mathrm{Tr}(\dot{\sigma}_R\hat{j}). \tag{6}$$

Since $\hat{j}$ is an off-diagonal operator only *off-diagonal* elements of $\dot{\sigma}_R$ enter W. So W and the potential drop, $V=W/J$, are governed by the inverse of the coherence lifetimes, Γ_{km}. This is an interesting result: since the current-carrying state is a coherent state, i.e., a state with finite off-diagonal elements in the density matrix, the work to be spent to sustain the current depends on the lifetimes of coherences and therefore has contributions from both depopulation and dephasing. In other terms, both elastic and inelastic scattering contribute to build up the molecular resistance since both of them disturb the coherent motion of electrons required for DC transport. On the other hand, only diagonal elements of $\dot{\sigma}_R$, i.e., only inelastic scattering events, contribute to $W_d = \mathrm{Tr}(\dot{\sigma}_R H_0)$, the power that the molecule dissipates to the environment. In general, for the adopted relaxation model,

W_d represents just a fraction of the total power, W, dissipated by the device so that some dissipation must occur at the leads. The molecular power balance, $\mathrm{Tr}(\dot{\sigma}_r H)=W+W_d$ is positive: the molecule heats as the current flows. Metallic leads are expected to provide good heat dissipation: whereas contacts are not explicitly modeled, I assume that they provide efficient dissipation as to guarantee for steady-state conditions and avoid molecular thermal decomposition.[26] Of course efficient energy dissipation is a prerequisite for steady-state DC transport,[4,10,11] but I avoid the calculation of the dissipated power since a reliable calculation of W_d would require a detailed model for relaxation processes occurring not only in the molecule but also in the leads. Instead the calculation of W, the electrical power spent on the molecule, only requires a model for the relaxation of *relevant* degrees of freedom. In this framework, the proposed approach applies to different regimes for transport. When dephasing dominates over depopulation [$\gamma'_{km} \gg (\gamma_{kk}+\gamma_{mm})/2$, the so-called coherent transport regime], the power dissipated in the molecule is negligible, $W_d=0$, and all the heat must be dissipated at electrodes. When depopulation rates become sizeable, instead, W_d is finite, but again, in general, the power balance is positive: the molecule dissipates some of the heat, but some dissipation occurs at the electrodes.

It is important to realize that the molecular relaxation dynamics is affected by electrical contacts. This is easily understood in single electron pictures: electrons are strongly scattered at the junctions and neither the elastic nor the inelastic lifetimes can be longer than the time required for the electron to cross the junction.[10] For correlated electrons $\dot{\sigma}_r$ describes the relaxation of molecular eigenstates and modeling the effects of leads on relevant lifetimes is more difficult. A detailed modeling is still lacking, here I just underline that even in the limit of very weak coupling, when electrons hardly hop from the molecule to the leads, the very same presence of a metallic surface close to the molecule opens new energy exchange channels then decreasing the inelastic lifetimes.[27–29] In the case of strong coupling, the blurring of the discrete molecular eigenstates as due to their mixing with the continuum of states of the metallic leads is responsible for large dephasing rates.[7] A particularly simple model for the relaxation matrix can be obtained in the strong coupling regime, when dephasing largely dominates on depopulation (coherent conductance regime). In the hypothesis that the effect of electrodes on relevant coherences is the same, one ends up with a very simple relaxation model with the same inverse lifetimes for all coherences: $\Gamma_{km}=\Gamma$. With this simple choice for the relaxation model, the electrical power spent on the molecule [Eq. (6)] reduces to $W=\lambda\Gamma J$, so that $V=\lambda\Gamma$ turns out proportional to Γ. In the following, when discussing junctions in the coherent conductance regime, Γ will be set to 1 (in units of $t/\hbar$): results for different Γ values can be easily obtained by a renormalization of V.

Figure 2 shows the characteristic curves calculated for a diatomic molecule with $\Gamma_{km}=1$. In the left panel results are shown for the symmetric, $\Delta=0$, system. As expected, electronic correlations decrease the conductivity. The curves in the right panel for an asymmetric system ($\Delta\neq 0$) show instead an increase of the low-voltage conductivity with increasing U. This result is related to the minimum excitation

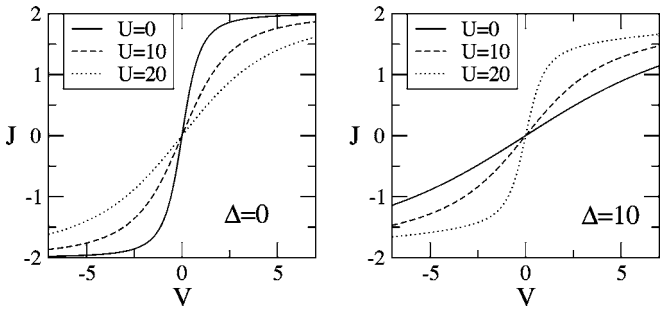

FIG. 2. Characteristic $J(V)$ curves for two-site two-electron junctions with different Δ and U. Depopulation and dephasing rates are set as to impose $\Gamma_{km}=1$.

gap, and hence the maximum conductance, of the system with $U=2\Delta$. The asymmetric diatomic molecule represents a minimal model for the Aviram and Ratner rectifier,[30] however, the characteristic curves in the right panel of Fig. 2 are symmetric, and do not support rectification. In agreement with recent results, rectification in asymmetric molecules is most probably due to contacts,[31] or to the coupling between electrons and vibrational or conformational degrees degrees of freedom.[32]

For the two site junction with $\Gamma_{km}=\Gamma$ a closed form for the zero-bias conductivity can be obtained within the proposed approach via a perturbative expansion of J, as follows:

$$\mathcal{G}_0=\frac{2}{\Gamma}\sum_k \frac{\langle k|\hat{j}|g\rangle|^2}{E_k-E_g}, \tag{7}$$

where g is the ground state of $H(0)$, with energy E_g, and the sum runs on all excited states. This expression coincides with the zero-frequency limit of the optical conductivity,[19] provided that the frequency ω appearing in the denominator of the expression for the optical conductivity in Ref. 19 is substituted by $\omega-i\Gamma$. Introducing a complex frequency to account for relaxation is a standard procedure in spectroscopy,[25] leading to similar effects as the introduction of an exponential switching on of the electromagnetic field:[19] in both cases Γ accounts for the loss of coherence of electrons driven by an electromagnetic field and properly suppresses the divergence of the optical conductivity due to the buildup of the phase of electrons driven by a static field. Of course, if relaxation is disregarded the DC limit of the optical conductivity diverges, in line with the vanishing of the molecular resistance in the absence of scattering.

Contacts represent an unavoidable source of scattering and set an upper limit to the conductivity.[3,7,10] Consider a single electron in a symmetric ($\Delta=0$) junction: the conductivity in Eq. (7) reduces to $\mathcal{G}_0=t/\Gamma$, where Γ is the inverse electronic lifetime. As pointed out by Das and Green,[10] contacts are efficient scattering centers and the electronic lifetime cannot be longer than the time required for the electron to cross the junction. Perturbation theory sets this time to $\tau=2\pi/t$, and one regains the standard expression for the maximum conductivity of an electron in a simple junction: $\mathcal{G}_0=e^2/h$. Whereas regaining the standard result gives confidence on the proposed approach, it is important to underline

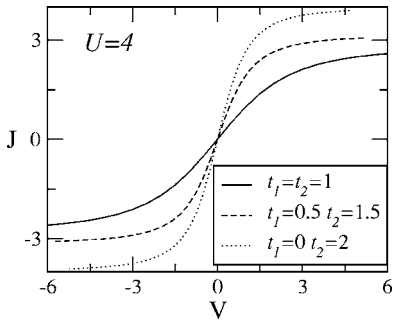

FIG. 3. Characteristic curves calculated for a three-atomic Hubbard chain with three electrons, equivalent sites ($\epsilon_i=0$), and the t_i in the figure. Depopulation and dephasing times have been chosen as to set $\Gamma_{km}=1$. These unphysical results have been obtained imposing a fixed average current [cf. Eq. (9)], and hence introducing a single Lagrange multiplier.

that this result is more general than usually understood.[3,5–7] The conductivity quantum was in fact derived for a dispersionless junction, i.e., an ideal junction where the only source of resistance is elastic scattering. On the contrary, our derivation is independent of the details of relaxation: it holds quite irrespective of the physical origin of Γ. In the above derivation Γ represents the inverse electronic lifetime and can have contributions from elastic and/or inelastic scattering, leading to a generalization of the conductivity quantum in line with recent results.[10,11]

III. LINEAR POLYATOMIC CHAINS

In a seminal paper on optical spectra of linear Hubbard chains[20] Maldague introduced the following real-space expression for the current operator of a Hubbard chain:

$$\hat{J} = -i\sum_{i,\sigma} t_i(c^{\dagger}_{i,\sigma}c_{i+1,\sigma} - \text{H.c.}). \tag{8}$$

Specifically, he adopted a similar approach to that proposed by Kohn[19] and applied a spatially uniform oscillating electric field by drawing a magnetic flux through the ring. Up to the first order in the vector potential the relevant Hamiltonian is[20]

$$H(\lambda) = H_0 - \lambda\hat{J}, \tag{9}$$

where λ measures the amplitude of the vector potential. This Hamiltonian coincides with the Hamiltonian proposed by Kosov[17] to describe DC transport in molecular wires and represents the real-space version of the invariant current-constrained approach by Mera *et al.*[12] Much as it occurs for diatomic molecules, also for linear polyatomic molecules the Lagrange-multiplier approach to DC transport corresponds to the low-field expansion of the Kohn Hamiltonian for a chain with periodic boundary conditions in a uniform electric field.

Equation (9) closely resembles Eq. (2) for the two-site molecule, and characteristic curves can be obtained along the same lines as described in the previous section. However, the Hamiltonian in Eq. (9) leads to unphysical results for DC transport in polyatomic molecules. Just as an example Fig. 3 shows characteristic curves calculated for a three-site Hubbard chain with three electrons, equivalent sites, constant average $t=(t_1+t_2)/2=1$, and increasing t-alternation $[0<(t_1-t_2)/2t<1]$. Results in Fig. 3 are obtained for a relaxation model with $\Gamma_{km}=1$. All other parameters fixed, the conductivity increases with increasing t-alternation, an unphysical result, particularly if one considers the limit of $t_2\rightarrow 0$, where, on physical grounds, one expects zero conductivity.

The failure of the Hamiltonian in Eq. (9) to describe DC transport is easily understood. $\hat{J}$ in fact measures the total current in the chain: at $t_2=0$ we calculate a finite J from the contribution of the first bond, whereas the current flowing through the second bond exactly vanishes. The average total current is the relevant quantity to optical spectroscopy, where we are interested in the electronic kinetic energy, but it is not the proper operator to describe DC transport. Indeed a steady state continuous current can be sustained in a circuit only if charges are conserved both at the global and local level. In other terms, the continuity constraint for DC transport requires that charge does not accumulate on atomic sites, a condition granted in linear molecules by imposing that the same amount of current flows in each bond. To impose this fundamental constraint a Lagrange multiplier must be introduced for each bond, as follows:

$$H(\lambda_i) = H_0 - \sum_i \lambda_i\hat{j}_i, \tag{10}$$

where $\hat{j}_i=-it_i\Sigma_\sigma(c^{\dagger}_{i,\sigma}c_{i+1,\sigma}-\text{H.c.})$, and the λ_i's are fixed by imposing $j_i=\langle G|\hat{j}_i|G\rangle=J$ independent of i. This Hamiltonian represents the real-space realization of uniform current constrained approaches.[12,16]

Before turning attention to characteristic curves, it is important to underline that imposing the continuity constraint, i.e., adopting the Hamiltonian in Eq. (10), rather than the average current Hamiltonian in Eq. (9), also affects the molecular properties. Figure 4 shows the J-dependence of the charge distribution in a three-site three-electron junction with $U=4$, different $\epsilon_i=-1,0,0$ and $t_i=1.5,0.5$. Left panels show the result obtained in terms of the total average current [i.e., adopting the Hamiltonian in Eq. (9)], the right panels show results obtained by properly imposing the continuity constraint [Hamiltonian in Eq. (10)]. In both cases the occupation number on atomic sites, n_i in the upper panels, tends towards the limit of 1 as the current increases, smoothing down the differences due to the mismatch of on-site energies. However, the behavior is different in the two cases, with particularly impressive differences in the low bias regime. Similarly, in the bottom panels, both the average bond order $(b=\langle b_1+b_2\rangle)$ and the bond-order alternation $\Delta b=\langle b_1-b_2\rangle)$ decrease with J, but again imposing the continuity constraint leads to a qualitatively different behavior. I stress that results in Fig. 4 are independent of the adopted model for relaxation dynamics.

Much as for the diatomic junction, the potential drop across the molecule is again calculated from the Joule law, as $V=W/J$, where W is the electrical work spent on the molecule to sustain the current J:

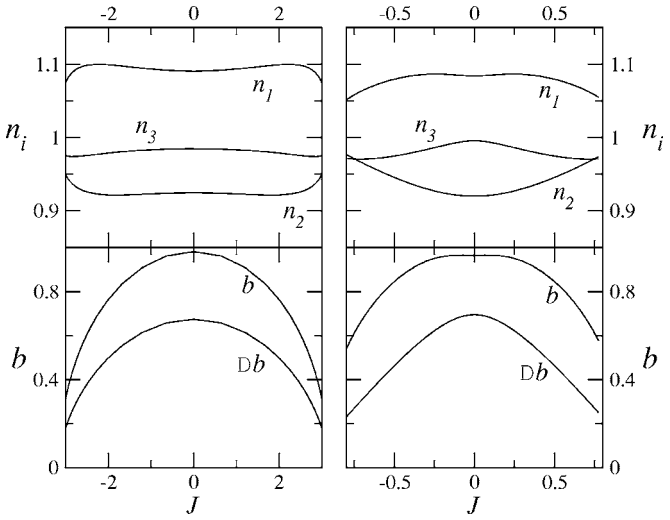

FIG. 4. The occupation numbers n_i, the average bond order b, and the bond-order alternation Δb shown as a function of the current flowing in a three-site chain with three electrons, $U=4$, $\epsilon_i=-1,0,0$ for $i=1,2,3$, respectively, $t_1=1.5$, and $t_2=0.5$. Results in the left panels are obtained in terms of the average total current according to the Hamiltonian in Eq. (9); results in the right panels are obtained imposing the continuity constraint, according to the Hamiltonian in Eq. (10).

$$W = -\sum_i \lambda_i \, \mathrm{Tr}(\hat{j}_i \dot{\sigma}_R). \tag{11}$$

Figure 5 shows the characteristic curves calculated for the same system as in Fig. 3, but using the Hamiltonian in Eq. (10), i.e., properly implementing the continuity constraint: as expected on physical grounds, the conductivity of the junction decreases with increasing t-alternation, and vanishes in the $t_2 \to 0$ limit: no current flows in a disconnected circuit.

The potential drop W in Eq. (11) naturally separates into bond contributions, with $W_i=-\lambda_i \, \mathrm{Tr}(\hat{j}_i \dot{\sigma}_R)$ measuring the work spent on the ith bond to sustain the current J through

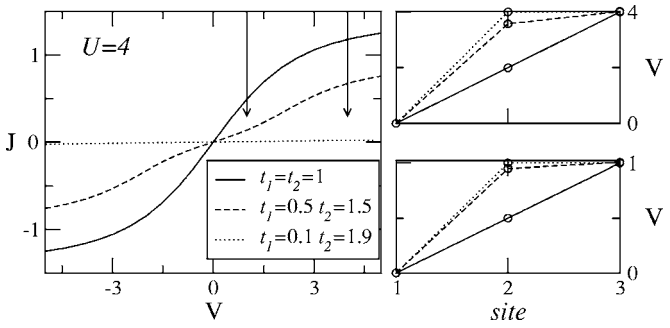

FIG. 5. Left panel: characteristic curves for a three-site chain with the same parameters as in Fig. 3 and the t-values in the figure. At variance with Fig. 3, results have been obtained introducing as many Lagrange multipliers as bonds [cf. Eq. (10)], as to guarantee for the continuity constraint. The arrows mark the V values corresponding to the potential profiles reported in the right panels. Right panels: the potential profiles calculated for the three junctions in the right panel at $V=4$ and $V=1$ (top and bottom panel, respectively).

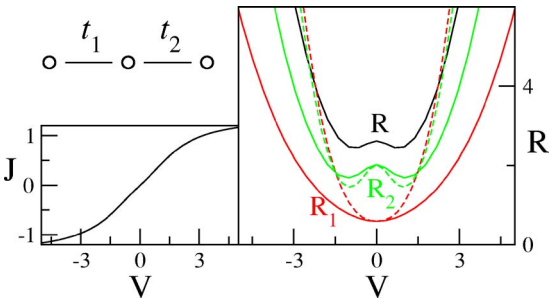

FIG. 6. (Color online) Left panel: characteristic curve for the three-site three-electron Hubbard molecule sketched in the figure, with $U=4$, constant on-site energies, $t_1=1.2$, $t_2=0.8$, $\Gamma_{km}=1$. Right panel: total (R) and bond resistances (R_1 and R_2). For bond resistances continuous and dashed lines show results obtained by allowing the current to flow through the whole molecule, and through a single bond, respectively.

the junction. Since, due to the continuity constraint, exactly the same current J flows through each bond, the total potential drop $V=W/J$ is the sum of the potential drops across each bond: $V=\Sigma_i V_i=\Sigma_i W_i/J$. This is a very important result: the continuity constraint, i.e., the local conservation of charge, can only be satisfied by imposing a specific potential profile across the junction. In the adopted real-space picture the total potential profile is obtained as the sum of the potential drops across each bond, as sketched in the right panels of Fig. 5. When the two bonds are equivalent, $t_1=t_2$ (continuous lines), the potential drops by the same amount across each bond, resulting in a linear potential profile. For nonequivalent bonds (either dashed or dotted lines) most of the potential drops at the weaker bond (more work must be spent on the weaker bond to sustain the current). It is interesting to stress that for low total voltages ($V=1$, lowest right panel) the potential profile calculated for the two cases with nonequivalent bonds is similar in spite of having fairly different t_i values. When increasing the total potential drop ($V=4$, upper right panel) the potential profile calculated for the system with $t_1=0.5$, $t_2=1.5$ (dashed lines) becomes less asymmetric. Indeed larger V imply larger perturbation in the Hamiltonian, reducing the effects of asymmetries in the molecular Hamiltonian.

The information on potential profiles can be conveniently conveyed in terms of bond resistances: $R_i=(\partial J/\partial V_i)^{-1}$, so that the potential drop across each bond is proportional to the relevant resistance. Figure 6 shows the results obtained for a three-site three-electron junction with $\Gamma_{km}=1$, $U=4$, equal on-site energies, and different t's. The left panel shows the characteristic $J(V)$ curve. Continuous lines in the right panel report the total resistance R, and the two bond resistances, R_1 and R_2. The molecular resistance varies with the applied voltage and, as expected, the resistance of the weaker bond is higher than the resistance of the stronger bond (the potential drop is larger across the weaker bond). As a direct consequence of the continuity constraint, the total resistance $R=(\partial J/\partial V)^{-1}$ is the sum of the two bond resistances, leading to a suggestive description of the linear molecule as an electrical circuit, with resistances associated with chemical bonds joint in series at the atomic sites. Whereas this picture is

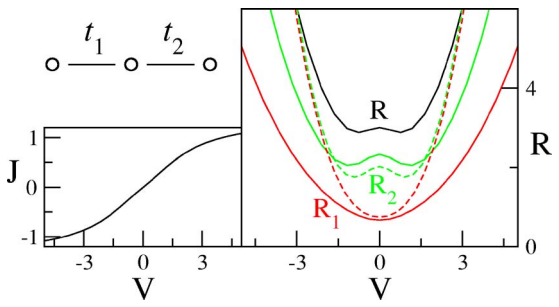

FIG. 7. (Color online) The same as in Fig. 6, but with a more complex relaxation model, defined by $\gamma_{km}=0.2$ (for $k>m$, low temperature limit) and $\gamma'_{km}=0.8$.

intriguing, the concept of bond resistance should be considered with care in molecular circuits. At variance with standard conductors, in fact, the resistance of the bonds depends not only on the circuit (the molecule) they are inserted in, but also on the way the resistances are measured. In fact the resistance of each bond can also be defined by forcing the current only through the specific bond [i.e., by setting a single $\lambda_i \neq 0$ in Eq. (10)]. Dashed lines in Fig. 6 show corresponding results. At zero bias, for each bond the two kinds of resistance do coincide so that the molecular resistance is the sum of the bond resistances measured by flowing current through each bond. This *additive* ohmic behavior for the zero-bias molecular resistance can be demonstrated by perturbative arguments for simple relaxation models as relevant to junctions in the coherent conductance regime, with $\Gamma_{km}=\Gamma$. This observation is in line with the observation of transmission rates inversely proportional to the molecular length for molecules in the same regime.[33] However, Fig. 6 clearly shows that additive behavior is rapidly spoiled at finite bias. Moreover, even at zero bias deviations from the additive behavior are observed for complex relaxation matrices with nonuniform Γ_{km}, as shown for a specific example in Fig. 7.

Multiple Lagrange multipliers account for nonlinear potential profiles in polyatomic molecules, in sharp contrast with the homogeneous electric field obtained by accounting for a single Lagrange multiplier,[17] or for a properly designed magnetic flux.[18–20] Modeling the potential profile as a linear function is a poor approximation for extended molecules.[34,35] Just as an example, in a four-atom four-electron molecule with exactly the same $t_i=1$ on each bond, the central bond is much weaker than the two external bonds leading to a ratio of the zero-bias resistances, R_2/R_1, ranging from 10 to 2 as U increases from 0 to 4. Largely nonlinear potential profiles are therefore expected even for highly idealized molecular structures.

Hubbard chains offer an oversimplified picture for molecular junctions, and cannot provide an accurate description of the behavior of specific systems. However, playing with toy models can help to understand some of the basic features of complex systems. A molecular junction is a complex object by itself, composed of a molecule (most often an organic molecule, with a main backbone of carbon atoms) and metallic leads contacting the molecule. The description of the molecule-lead contact is a delicate problem that, in a toy-model approach, can be simplified in terms of a four-site

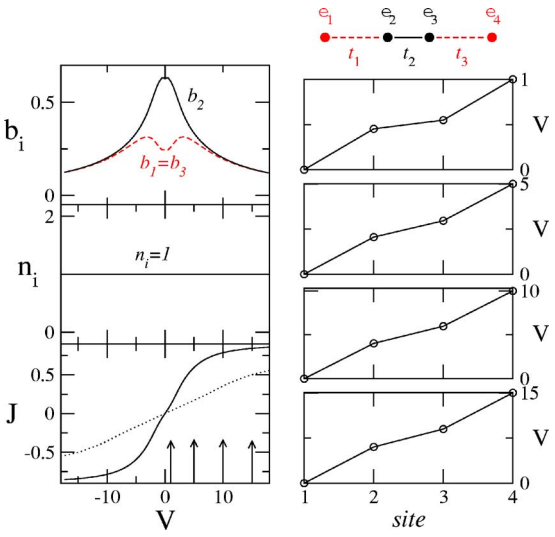

FIG. 8. (Color online) Results for the four-site junction sketched in the figure, with four electrons, $\Gamma_{km}=1$, $t_1=t_3=0.5$, $t_2=1$, and $\epsilon_i=0$. From top to bottom the three left panels shows bond orders, on-site occupation numbers, and the current vs the applied potential drop. The dotted line in the bottom left panel shows the characteristic curve obtained without imposing the continuity constraint. The arrows in the same panel mark the V values corresponding to the potential profiles shown in the right panels. The right panels show the potential profiles relevant to four different values of the total potential drop: from top to bottom $V=1$, 5, 10, and 15.

Hubbard junction where the two central sites describe the molecule and the two external sites mimic atoms from leads. Accordingly, Figs. 8 and 9 report results obtained for four-site junctions with a strong ($t=1$) central (molecular) bond and two weaker ($t=0.5$) lateral (molecule-lead) bonds. In Fig. 8 the two external sites have the same energy as the inner ones, whereas in Fig. 9 the external (lead) sites have a much lower energy than the internal (molecular) ones as to mimic the different Fermi energies or to account for an applied gate voltage.[36] For $\epsilon_i=0$ (Fig. 8) electron-hole symme-

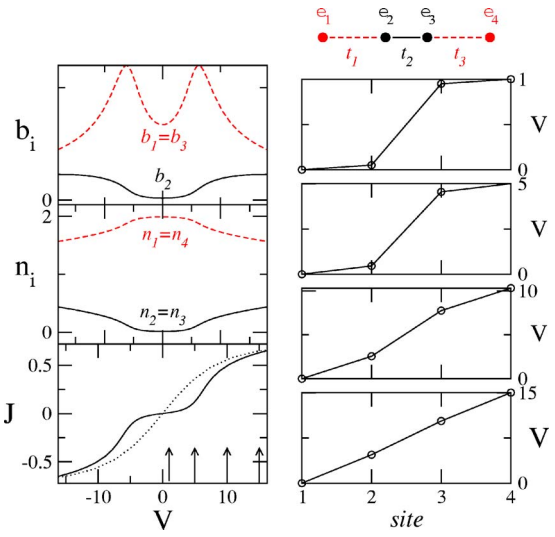

FIG. 9. (Color online) The same as in Fig. 8 but with $\epsilon_1=\epsilon_4=-10$, $\epsilon_2=\epsilon_3=0$.

try fixes the occupation number $n_i=1$. However, due to the smaller t's, the two later bonds are weaker than the central bond and most of the potential drop occurs at the lead-molecule contact. Of course as V increases, i.e., as the perturbing field increases, the details of the unperturbed Hamiltonian become less important, the bond orders equalize and the potential profile becomes almost linear. The case of non-equivalent sites in Fig. 9 is more interesting. Due to the mismatch of on-site energies, at zero bias almost all electrons are located at the external (leads) sites: $n_2=n_3\sim 0$ and $n_1=n_4\sim 2$. The circuit is almost open ($b_2\sim 0$) with a huge resistance. In these conditions the potential profile is largely nonlinear: most of the potential drop is found at the central bond (cf. the two uppermost right panels in Fig. 9). At larger V the conductivity [i.e., the slope of the $J(V)$ curve] increases. In fact, large V implies large perturbing fields, λ_i's, in the Hamiltonian in Eq. (10). In these conditions the high energy eigenstates of the unperturbed Hamiltonian with a sizable occupation of central (molecular) sites contribute to the perturbed (current carrying) ground state, $|G(\lambda)\rangle$. Accordingly, in Fig. 9 at large V the occupation of molecular sites ($n_2=n_3$) as well as the central bond order (b_2) become significantly different from zero, leading to a decrease of the resistance in the central bond and hence to a decrease of the total resistance. This behavior is consistent with the picture emerging from a VC description: in systems with a large mismatch of Fermi energy a large bias must be applied to the junction for the electrons being able to travel across the barrier. The connection between V and the Lagrange multipliers is not direct in CC approaches, but goes through the relaxation times. Roughly speaking V goes with the λ_i's times the inverse coherence lifetime of relevant states: if coherences decay rapidly, as due to either elastic or inelastic scattering, more power has to be dissipated to sustain the current, and larger V are needed to overcome the larger resistance. But again, this is consistent with the standard VC picture that predicts large resistances in systems with short lifetimes.

The dotted lines in the lower left panels of Figs. 8 and 9 show the characteristic curves calculated for the same model without imposing the continuity constraint, i.e., adopting the Hamiltonian in Eq. (9). At zero bias the Hamiltonians relevant to the two models are obviously the same, so that at $V=0$ exactly the same charge distribution is obtained for the two models. The zero bias conductivity is, however, very different: as stressed above, the current calculated without imposing the continuity constraint describes an average current and not a coherent flux of charges along the junction.

Before closing this section lets sketch the treatment of a slightly more complex model, where a next-nearest-neighbor hopping t' is added to the Hamiltonian for a three site junction. This opens a new channel for electrical transport, and a term $-\lambda'\hat{j}'$ adds to the Hamiltonian with $\hat{j}'=-it'\Sigma_\sigma(c_{1\sigma}^\dagger c_{3\sigma}-\text{H.c.})$. Continuity imposes $j_1=j_2$, and the total current flowing through the molecule is $J=j_1+j'$. Of course, j' is not constrained by continuity. However, the potential drop across the molecule, i.e., the potential drop measured at sites 1 and 3, must be uniquely defined. Therefore λ_1, λ_2, and λ' must be tuned as to satisfy: (a) $j_1=j_2$, and (b) $V_1+V_2=V'=V$, with $V_i=W_i/j_i$ and $V'=W'/j'$. Imposing a constraint on the potentials involves in general a fairly tedious trial and error procedure, but becomes trivial for systems with $\Gamma_{km}=\Gamma$. In this case in fact $V_i=\Gamma\lambda_i$ and $V'=\Gamma\lambda'$: the constraint on the potentials immediately translates into a constraint on the Lagrange multipliers. Figure 10 shows some results obtained in the coherent conductance limit for a system with $t_1=t_2=1$, $t'=0.4$. In spite of the fairly large t' value, the contribution to the current from the bridge-channel is small, mainly due to the small bond order for next-nearest-neighbor sites. Once again, the physical constraints imposed to currents and potentials lead to standard combination rules for bond resistances with $1/R=1/R'+1/(R_1+R_2)$. As for DC transport, the molecule behaves as an electrical circuit with two resistances, R_1 and R_2 in series bridged by a parallel resistance, R'.

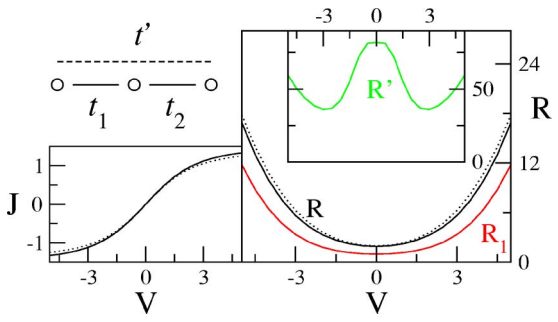

FIG. 10. (Color online) Left panel: characteristic curves of the three-site three-electron junction sketched in the figure, with $U=4$, $t_1=t_2=1$, constant on-site energies, and $\Gamma_{ij}=1$. Continuous and dotted lines refer to $t'=0.4$ and 0, respectively. Right panel: molecular and bond resistances for the chain with $t'=0.4$. The dotted line shows the total resistance for the chain with $t'=0$.

IV. DISCUSSION AND CONCLUSIONS

Current and voltage constrained approaches to molecular junctions offer complementary views of the same phenomenon and, each one having its merits and drawbacks, both should be carefully explored to reach a comprehensive representation of the complex physics of molecular transport. One of the most appealing features of CC approaches is the possibility to work with correlated electrons. Here I fully exploit this opportunity combining the CC description of transport with a real-space description of the molecule. The resulting picture is strongly rooted in the concept of chemical bond: chemical bonds offer channels for electronic transport, i.e., the current flows through the bonds. This view should be contrasted with the more familiar picture of electrons flowing through molecular orbitals, as resulting from the typically one-electron description of molecular junctions adopted in VC approaches. None of the two pictures is more fundamental nor more correct than the other: they correspond and actually steam from the two complementary and equally fundamental descriptions of molecular binding as based on the molecular orbital or valence bond descriptions.[37] Both are important and should be known to fully appreciate the complex realm of molecular physics. The description of molecular junctions is a complex problem, and this contribution just

represents a first effort towards the development of a real-space picture for molecular transport: many problems are still open, and the picture can be improved in several respects. However, several interesting concepts and a few safe results emerge that can deepen current understanding of the problem.

One of the open problems in CC approaches is the definition of the the voltage drop needed to sustain the current. Energy conservation, as stated by the Joule law, sets the problem: the potential drop can be calculated, in a system with fixed current, from the electrical work spent on the junction. The idea is simple and underlines the physical connection between the applied voltage (and hence the molecular resistance) and relaxation (scattering) phenomena occurring in the molecule: any model for molecular transport must include a model for relaxation or scattering. Here I adopt a general phenomenological model for relaxation dynamics as described in the language of reduced density matrix.[24,25] It turns out that the molecular resistance is governed by the relaxation of off-diagonal matrix elements (coherences) of the density matrix: the relevant lifetimes are due to both dephasing and depopulation, i.e., both elastic and inelastic scattering contribute to the resistance. The model for relaxation dynamics is general: when depopulation rates are negligible with respect to dephasing rates it applies to systems where no dissipation occurs within the molecule and henceforth all power is dissipated at leads. For sizable or large depopulation rates the model describes junctions where at least some dissipation occurs within the molecule. The model is, however, phenomenological:[24,25] a microscopic model for the relaxation dynamics properly accounting for the effects of contacts is an important open issue. Indeed just for the special case of a single electron in the simplest two-site junction a maximum value for the electronic lifetime is fixed by simple physical considerations[10] and in this specific case the well-known result for quantized conductivity is regained. Quite interestingly the result is more general than originally understood, as it applies to dispersionless as well as dispersive junctions.

Two versions of CC approaches have been suggested:[12] the invariant CC method where the total current is fixed in the junction, and the constant CC method where the local current is fixed. The first approach leads to a simple Hamiltonian where a single Lagrange multiplier, coupled to the total current, appears. Incidentally, this Hamiltonian represents the low-field expansion of the Hamiltonian that describes the junction in a magnetic flux.[19,20] This approach, however, does not satisfy the basic continuity constraint for DC transport and, as discussed in Sec. III, leads to unphysical results. To properly enforce the continuity constraint, one must control the *local current*, i.e., in the adopted real space representation, the current flowing through each single bond. This detailed control requires the introduction of a Lagrange multiplier for each bond. Multiple Lagrange multipliers naturally result in nonlinear potential profiles for polyatomic molecules, in sharp contrast with the spatially homogeneous electric field implied in CC approaches where a single Lagrange multiplier is introduced, or even when the current is imposed on the junction by driving a magnetic flux through the circuit.[18–20] Of course working with multiple Lagrange multipliers, and even more the need for implementing several constraints, make the approach not particularly well-suited to be integrated with a detailed quantum chemical description of the molecular junction. The approach is instead easily implemented in real-space or quantum-cell Hamiltonians for the junction, and offers the intriguing possibility to account for nonadiabatic vibrations.

In conclusion, an approach is presented for the calculation of characteristic current/voltage curves for molecular junctions avoiding any reference to electronic reservoirs. A steady-state current is imposed on the molecule prepared in a nonequilibrium state, and the voltage drop is obtained from the electrical power spent on the molecule to sustain the current. Molecular resistance is related to relaxation of molecular states as due to both elastic and inelastic scattering (i.e., depopulation and dephasing). Molecular relaxation is described in terms of a phenomenological model borrowed from the field of molecular spectroscopy. The exchange of concepts and techniques between the mature field of molecular spectroscopy and the new field of molecular transport is an interesting feature of the proposed approach. However, specific features of molecular junctions must also be underlined: the continuity constraint for steady-state DC current has no counterpart in molecular spectroscopy and is responsible for the appearance of nonlinear potential profiles in extended molecules, in sharp contrast with the spatially homogeneous electric fields of molecular spectroscopy. In the adopted real-space picture, the implementation of the continuity constraint results in the concept of bond resistance, in a suggestive description of the molecule as an electrical circuit with current flowing through chemical bonds.

ACKNOWLEDGMENTS

I thank D. Kosov, and F. Green for useful discussions and correspondence. Interesting discussions with A. Girlando, S. Pati, S. Ramasesha, and Z.G. Soos are acknowledged, as well as contributions from S. Cavalca and C. Sissa. Work supported by Italian MIUR through FIRB-RBNE01P4JF and PRIN2004033197-002.

*Electronic address: anna.painelli@unipr.it

[1] *Introducing Molecular Electronics*, edited by G. Cuniberti, G. Fagas, and K. Richter, Lecture Notes in Physics, Vol. 680 (Springer, Berlin, 2005).

[2] C. Joachim and M. A. Ratner, Proc. Natl. Acad. Sci. U.S.A. **102**, 8800 (2005).

[3] A. Nitzan and M. A. Ratner, Science **300**, 1384 (2003).

[4] C. Bustamante, J. Liphardt, and F. Ritort, Phys. Today **58-7**, 43 (2005).

[5] M. Buttiker, Phys. Rev. B **32**, 1846 (1985).

[6] R. Landauer, IBM J. Res. Dev. **1**, 223 (1957).
[7] S. Datta, Nanotechnology **15**, S433 (2004).
[8] A. Kamenev and W. Kohn, Phys. Rev. B **63**, 155304 (2001).
[9] F. Sols, Phys. Rev. Lett. **67**, 2874 (1991).
[10] M. P. Das and F. Green, J. Phys.: Condens. Matter **15**, L687 (2003).
[11] M. P. Das, F. Green, and J. S. Thakur, Phys. Rev. Lett. **92**, 156804 (2004).
[12] H. Mera, P. Bokes, and R. W. Godby, Phys. Rev. B **72**, 085311 (2005).
[13] M. D. Ventra and T. N. Todorov, J. Phys.: Condens. Matter **16**, 8025 (2004).
[14] T. K. Ng, Phys. Rev. Lett. **68**, 1018 (1992).
[15] W. Magnus and W. Schoenmaker, Phys. Rev. B **61**, 10883 (2000).
[16] D. S. Kosov, J. Chem. Phys. **116**, 6368 (2002).
[17] D. S. Kosov, J. Chem. Phys. **120**, 7165 (2004).
[18] K. Burke, R. Car, and R. Gebauer, Phys. Rev. Lett. **94**, 146803 (2005).
[19] W. Kohn, Phys. Rev. **133**, A171 (1964).
[20] P. F. Maldague, Phys. Rev. B **16**, 2437 (1977).
[21] E. Y. Loh, D. K. Campbell, and J. T. Gammell, in *Interacting Electrons in Reduced Dimensions*, edited by D. Baeriswyl and D. K. Campbell, NATO-ASI Series B: Physics (Plenum Press, New York, 1988), Vol. 213, p, 91.
[22] Z. G. Soos and S. Ramasesha, in *Valence Bond Theory and Chemical Structure*, edited by D. J. Klein and N. Trinajstic (Elsevier, New York, 1990).
[23] M. DiVentra, Y.-C. Chen, and T. N. Todorov, Phys. Rev. Lett. **92**, 176803 (2004).
[24] S. Mukamel, *Principles of Nonlinear Optical Spectroscopy* (Oxford University Press, New York, 1995).
[25] R. W. Boyd, *Nonlinear Optics* (Academic Press, New York, 2003).
[26] A. Nitzan, Annu. Rev. Phys. Chem. **52**, 681 (2001).
[27] M. R. Philpott, J. Chem. Phys. **62**, 1812 (1975).
[28] R. R. Chance, A. Prock, and R. Silbey, Adv. Chem. Phys. **37**, 1 (1978).
[29] M. Galperin and A. Nitzan, Phys. Rev. Lett. **95**, 206802 (2005).
[30] A. Aviram and M. A. Ratner, Chem. Phys. Lett. **29**, 274 (1974).
[31] F. Zahid, A. W. Ghosh, M. Paulsson, E. Polizzi, and S. Datta, Phys. Rev. B **70**, 245317 (2004).
[32] A. Troisi and M. A. Ratner, J. Am. Chem. Soc. **124**, 14528 (2002).
[33] W. B. Davis, M. R. Wasielewski, M. A. Ratner, V. Mujica, and A. Nitzan, J. Phys. Chem. A **101**, 6158 (1997).
[34] G. C. Liang, A. W. Ghosh, M. Paulsson, and S. Datta, Phys. Rev. B **69**, 115302 (2004).
[35] O. Berman and S. Mukamel, Phys. Rev. B **69**, 155430 (2004).
[36] Y. Asai and H. Fukuyama, Phys. Rev. B **72**, 085431 (2005).
[37] I. N. Levine, *Quantum Chemistry* (Prentice-Hall, Englewood Cliffs, NJ, 1991).